JOURNAL OF GEOPHYSICAL RESEARCH, VOL. 113, C07010, doi:10.1029/2007JC004393, 2008



# Warming of SST in the cool wake of a moving hurricane

James F. Price,[1] Jan Morzel,[2] and Pearn P. Niiler[3]

Received 14 June 2007; revised 17 December 2007; accepted 7 April 2008; published 8 July 2008.

[1] Satellite imagery and in situ ocean data show that the cool anomaly of sea surface temperature in the wake of a moving hurricane will disappear over an e-folding time of 5 to 20 days. We have constructed a very simple, local model of the warming process by evaluating the heat budget of the surface layer. This requires (1) an estimate of the heat flux anomaly, $\delta Q$, that we presume is associated with the cool anomaly of sea surface temperature (SST), $\delta Q = \lambda\, \delta T$, where $\delta T$ is the SST anomaly and for nominal trade wind conditions, $\lambda = -65$ W m$^{-2}$ C$^{-1}$, and (2) the thickness, $D$, of the surface layer that absorbs this heat flux anomaly. Evidence from numerical simulations is that $D$ is the trapping depth of the diurnal cycle, and from existing models we estimate $D = c_1\tau/Q_n^{1/2}$, where $\tau$ is the wind stress magnitude, $Q_n$ is the diurnal maximum (noon) heat flux and $c_1$ is a product of known physical constants. The cool anomaly is then a decaying exponential, $\delta T \propto \delta T_0 \exp(-t/\Gamma)$, where $\delta T_0$ is the spatially dependent cooling amplitude, and the e-folding time is $\Gamma = c_2\tau/\lambda Q_n^{1/2}$, with $c_2$ also known. This solution agrees reasonably well with the observed e-folding time of cooling in the wake of Hurricane Fabian (2003), approximately 5 days, and in the wake of Hurricane Frances (2004), very roughly 20 days. The latter e-folding time was greater (i.e., the normalized warming rate was slower) primarily because winds were fresher and secondarily because cloud cover was greater. It is notable that the e-folding time in this solution depends upon two properties of the surface heat flux, the slowly varying heat flux anomaly and the diurnal variation of the heat flux, here represented by the noon maximum, $Q_n$.

**Citation:** Price, J. F., J. Morzel, and P. P. Niiler (2008), Warming of SST in the cool wake of a moving hurricane, *J. Geophys. Res.*, *113*, C07010, doi:10.1029/2007JC004393.

## 1. Cool Wakes

[2] Moving hurricanes leave behind a cool wake within which the sea surface temperature (SST) is reduced by typically 2° to 4°C [*Stramma et al.*, 1986]. Hurricane-induced cooling of SST is thought to be one of several factors that determine the intensity of a hurricane, with greater cooling contributing to reduced hurricane-ocean heat flux and thus to reduced hurricane intensity [*Emanuel et al.*, 2004; *Lin et al.*, 2005]. This aspect of hurricane-ocean interaction is an important, practical motive for studying the cool wake phenomenon [see also *Sriver and Huber*, 2007], but it is not the main topic here. Rather, while analyzing cool wakes seen in satellite imagery and in situ data, we have been struck by what is oftentimes a rapid warming and thus a rapid disappearance of the cool wake. In the Fabian (2003) case studied here there was significant warming of the wake within 5 days of the hurricane passage (e-folding of the cool anomaly). In a second case studied here, Frances (2004), appreciable warming required about 20 days. *Nelson* [1998] reported a case of significant warming in about 10 days following a Sargasso Sea hurricane.

[3] This warming phenomenon has some practical consequences for the use of satellite imagery to infer SST cooling, namely, satellite data acquired more than a day or two after a hurricane passage are likely to underestimate the cooling that occurred underneath the hurricane and that could have contributed to hurricane-ocean interaction. While the SST signature of a hurricane wake may disappear fairly quickly from satellite imagery, the subsurface signature of a cool wake (deeper than about 25 m) likely persists as a thermal anomaly, cooler within the relic mixed layer and warmer in the upper seasonal thermocline, for at least a few weeks. Successive hurricanes will thus encounter oceanic conditions that are less favorable for intensification than the observed SST and thermocline climatology would imply. There are larger, scientific reasons to study this phenomenon as well. In this paper we are led to consider some of the physical differences in the upper ocean response to cooling and wind-mixing, which form a hurricane cool wake in the first place, and the subsequent response to warming and fair weather conditions that act to erase a cool wake.

[1]Physical Oceanography Department, Woods Hole Oceanographic Institution, Woods Hole, Massachusetts, USA.
[2]CoRA Division, NorthWest Research Associates, Boulder, Colorado, USA.
[3]Scripps Institution of Oceanography, University of California, San Diego, La Jolla, California, USA.


0148-0227/08/2007JC004393$09.00

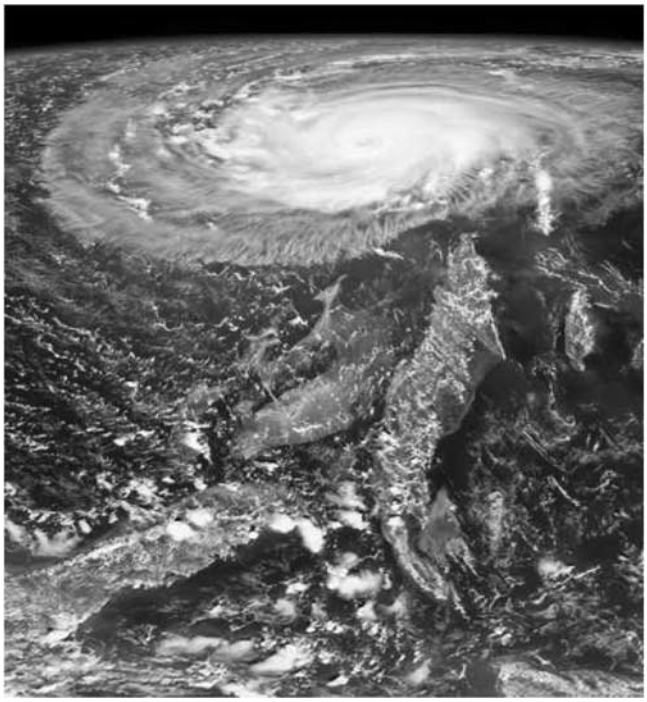

**Figure 1.** Hurricane Frances on 1 September 2004, near the site of the CBLAST field experiment. Frances was then a category 3–4 hurricane and was moving toward the viewer at about 5 m $s^{-1}$. Frances continued along a west northwest path and made landfall in Florida. This image was made by NASA SeaWiFS, http://daac.gsfc.nasa.gov/gallery/frances/#SeaWiFS, from a position over the Gulf of Mexico and looking toward the east southeast.

### 1.1. CBLAST Hurricanes Fabian and Frances

[4] Our study is based upon observations of the ocean response to two western North Atlantic hurricanes; Hurricane Fabian (September 2003) that was the object of the CBLAST-High pilot field program and Hurricane Frances (September 2004; Figure 1), the object of the intensive CBLAST field program in 2004. Both of these hurricanes formed in the central trade wind region and then moved westward along a latitude of about 18°N. Hurricane Fabian turned northward as it approached the Leeward Islands and struck Bermuda on 2 September as a large and powerful category 3–4 hurricane; Hurricane Frances, also a large and powerful hurricane, continued along a more westward path that crossed the southern Bahamas and made landfall in Florida. Relevant satellite imagery of these storms may be found at http://www.nasa.gov/vision/earth/environment/hurricane_bloom.html and http://www.nasa.gov/vision/earth/lookingatearth/Frances_Roars.html.

[5] A sequence of GOES SST images of the CBLAST 2003 and the 2004 field regions is in Figures 2 and 3 (a much longer sequence of color images is available in the auxiliary material[1]). In both cases the prehurricane SST was fairly homogeneous (aside from very near the islands in the Frances case) and about 29°C, typical of late summer in this region. A cool wake is clearly evident behind both hurricanes; there was significant cooling over a width of several hundred kilometers and a maximum amplitude of cooling up to 4°C. Within a given image, the cooling of SST is usually greatest immediately behind a moving hurricane and decreases with distance back along the track. Successive daily images of SST show that the cool wake warmed with time after the hurricane passage, the topic of this paper.

### 1.2. The Goal and the Plan

[6] Our broad goal is to develop an understanding of the air-sea interaction processes that lead to the (sometimes) rapid warming of SST in the cool wake of a hurricane. A specific goal is to describe and interpret the wake warming observed in the CBLAST field data, in situ measurements of SST by surface drifters and GOES-derived SST imagery, starting in section 2. In section 3 we make an objective estimate of the warming rate using satellite and drifter data where available (the Fabian case) or drifter data alone (the Frances case). As we have already noted, the rate of warming was quite different between these two cases; there was appreciable warming of the wake of Hurricane Fabian within about 5 days of the hurricane passage, while in the Frances case, appreciable warming required about 20 days (e-folding time of the cool anomaly, sections 3.2 and 3.3). Several characteristics of the wake warming suggest that the warming process is mainly local, i.e., depth and time-dependent, and that is driven by surface fluxes (section 3.4). This suggests numerical simulations of a storm-punctuated, tradewind atmosphere imposed upon a one-dimensional upper ocean model (section 4.1). Our goal for the modeling is to derive an explicit parameter dependence of the e-folding time, section 4.2, and so to offer an explanation of the difference between the Fabian and Frances cases. The final section, section 5, gives a summary of the main results and our closing remarks.

## 2. In Situ and Remote Observations From the CBLAST Experiments

### 2.1. Surface Drifter Data

[7] The 2003 CBLAST pilot field program included the air deployment of eight surface drifters in a compact, linear array that spanned the track of Hurricane Fabian around latitude 26°N (Figure 4). These drifters measured temperature at a depth of 10 cm (hereafter, "drifter SST") with higher consistent temporal resolution than does satellite imagery. These drifter SST data also show that the cool wake in SST was largely erased by warming within about 5 days after the passage of Fabian. But then starting on day 255, the warming trend was reversed. This abrupt change in the evolution of SST was coincident with an increase of wind speed in the CBLAST region that accompanied the passage of Hurricane Isabel about 300 km to the south of the CBLAST region (Figures 2 and 6). The GOES images (Figure 2) show that the SST cooling in the wake of Fabian reappeared at that time. Thus, warming of the cool wake acted to reduce the spatial variability of SST by preferentially warming the coolest regions, a point made by *Katsaros and Soloviev* [2004]. On the other hand, the wind-mixing that began on day 255 acted to increase SST

[1] Auxiliary materials are available in the HTML. doi:10.1029/2007JC004393.

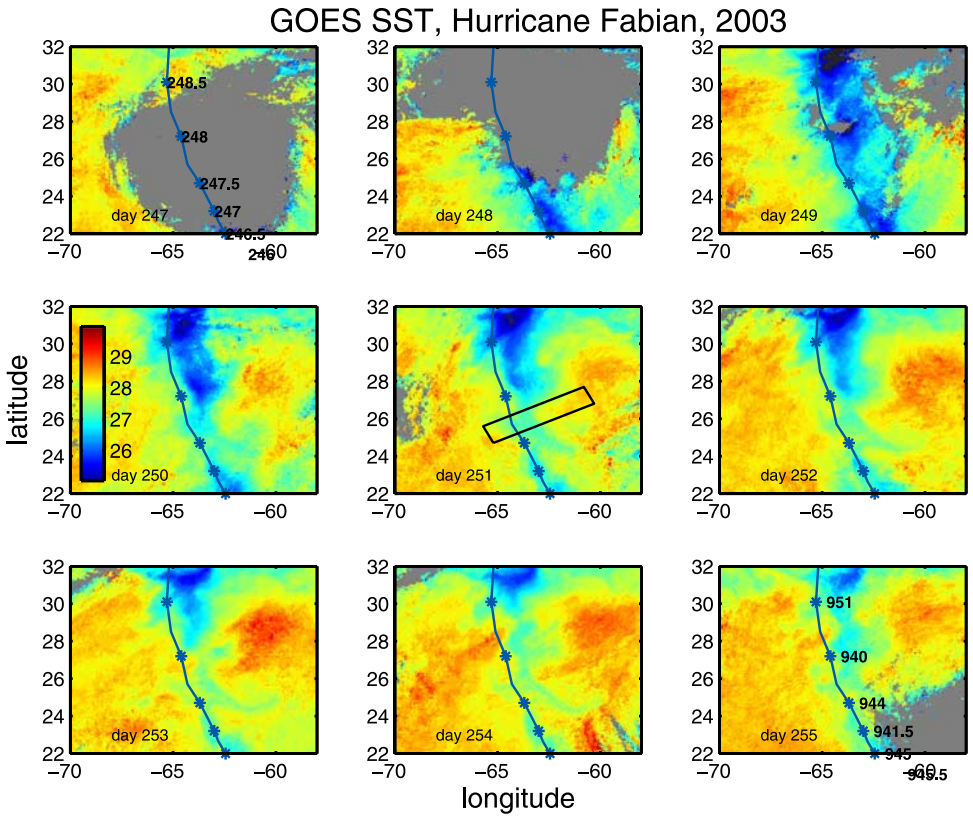


**Figure 2.** GOES SST images at daily intervals showing the passage of Hurricane Fabian through the central Sargasso Sea. The year day is shown in the lower left of each image. Hurricane Fabian is in the center of the image field on day 247, 4 September 2003. Bermuda is just above the northern edge of the region shown here and directly beneath the track of Fabian, whose track is the thin black line running roughly south to north. The eye location at half-day intervals is noted by the asterisks labeled with the year day (upper left) and central pressure (mbar) is noted on the lower right (track data are from the Johns Hopkins University online archive). Clouds are the uniform gray mass and SST is color-coded by the scale at left middle. The CBLAST region that is sampled for SST is shown as the rectangle in the center (more on this in section 3.2). Hurricane Isabel was just entering the southeast corner of the image field on the last day shown, 255, and continued almost due westward. Isabel caused enhanced wind speeds in the CBLAST region starting from day 255, when, notice, the SST cooling in the wake of Fabian reappeared.

spatial variability by uncovering the subsurface thermal associated with the subsurface part of Fabian's cool wake.

[8] The drifter data reveal that the wake warming was strongly modulated by the diurnal cycle. On some days the diurnal cycle of SST had an amplitude $T'$ in excess of 1°C, but the amplitude was quite variable from day-to-day. On a given day, the amplitude of the diurnal cycle of SST was often variable in space even over the small, O(100 km), scale of the drifter array. The ensemble (time and space) average amplitude of the diurnal cycle was $\langle T' \rangle = 0.58$°C and the standard deviation was 0.30°C. The significant amplitude of the diurnal cycle is evidence that the solar insolation was strong, i.e., that skies were clear, as is evident also in GOES imagery and that wind speeds were fairly low (more on this in section 2.3) [*Price et al.*, 1986; *Gentemann et al.*, 2003].

[9] The 2004 CBLAST intensive field program collected a wide range of ocean in situ observations [*Black et al.*, 2007] some of which has been reported by *Sanford et al.* [2007] and by *D'Asaro et al.* [2007]. The 2004 CBLAST data set includes more than 40 surface drifters that were operating in the vicinity of the path of Hurricane Frances. Some of these surface drifters were air-deployed a day in advance of Hurricane Frances as part of the 2004 field program and others were deployed weeks or months in advance as part of an ongoing, operational forecasting program (sponsored by the U. S. Naval Oceanographic Office). Of the total, 25 surface drifters were within 200 km of the CBLAST field program center, just north of Hispaniola (Figure 1) near longitude 70°W, and are most useful for the present purpose (more on these drifter data in section 3.2).

### 2.2. GOES Imagery

[10] The GOES SST data used here are daily composites having 6 km horizontal resolution and that were supplied by the POET data server, http://poet.jpl.nasa.gov//. The estimated error on a single retrieval by GOES is rather high, two times rms = 0.7°C (reported on the POET Web server noted above) which is consistent with our comparison with

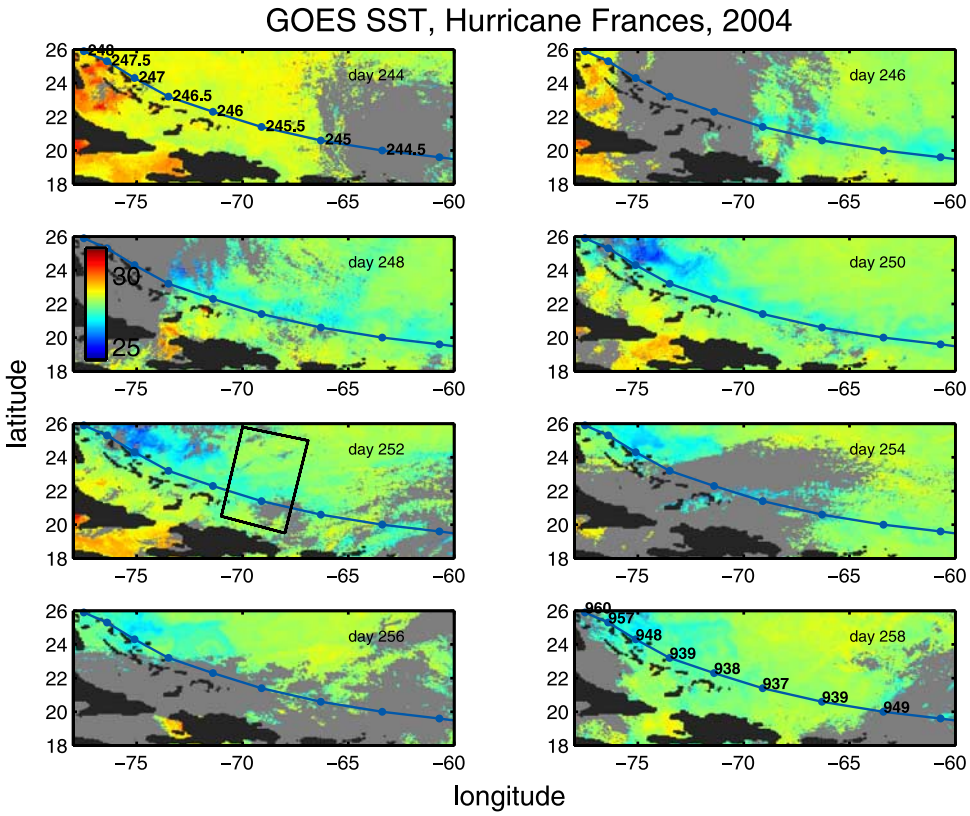


**Figure 3.** GOES images at 2 day intervals showing the passage of Hurricane Frances along a path just north of the Leeward Islands. The year day is shown at upper left; day 244 was 31 August 2004. Central pressure (mbar) is at lower right. The color scale for SST is shown on day 248, and the CBLAST region is shown as the black rectangle. Notice that there was fairly extensive cloud cover on many days; the clouds on day 254 are associated with Hurricane Ivan, which passed through the central Caribbean Sea on day 255, and the clouds on day 258 were a precursor of Hurricane Jeanne, which passed through the CBLAST region on 16 September, just after the last image shown here.

drifter SST data (Figure 5). The reason for this comparatively high noise level is, in part, that the GOES satellite measures in a smaller number of infrared channels than do AVHRR imagers. In compensation, the GOES images are daily composites (averages of the cloud-free regions) made from hourly measurements and hence are able to see around some smaller, several kilometer-scale cloud features that are often present in trade wind regions and the outlying region of a hurricane; see the SeaWiFS image of Frances in Figure 1. Thus there is a great deal more SST data reported by GOES than from AVHRR imagers. However, there are instances wherein anomalous (cool or warm) SSTs are reported near the edge of obvious, identified cloud masses and other instances wherein a cloud mass in one image becomes a cloud-like pattern of anomalous SST in the next image. These problems are well known for GOES, and the upshot is that when we try to infer quantitative results from an analysis of GOES images it is necessary to average over an extensive set of GOES data, and, even then, it is helpful to keep an eye on the individual images. The weather conditions post-Fabian included nearly clear skies and good viewing conditions for GOES. By comparison, the cloud cover was much higher post-Frances, obscuring the sea surface on about half the possible days. In that case we rely mainly upon the extensive surface drifter SST data set.

#### 2.2.1. Horizontal Pattern of SST Cooling: Across-Track Variation

[11] Perhaps the most impressive qualitative feature of this and most other SST imagery of hurricane wakes is that the cool wake was significantly biased to the right side of the hurricane track (looking in the direction of the hurricane motion; Figures 2 and 3). The coolest SST in the wake of Fabian in the CBLAST region was about 80 km to the right of the track (see also Figure 4); in the wake of Frances the coolest SST was about 70 km to the right of the track. These distances are very roughly twice the radius to the maximum winds, about 30 km in Fabian and about 40 km in Frances. A similar rightward bias of SST cooling has been observed consistently for moderately or rapidly moving hurricanes, $U_h \geq 4$ m s$^{-1}$ [*Stramma et al.*, 1986; *Cornillon et al.*, 1987; *Nelson*, 1998]. A rightward bias is less pronounced under very slowly moving hurricanes [*Lin et al.*, 2003b] and, in the limit that a hurricane is stationary, there is no left or right and consequently no left-to-right bias whatever. The rightward bias of cooling in the wake of moving hurricanes has been attributed to the asymmetric turning (in time) of wind

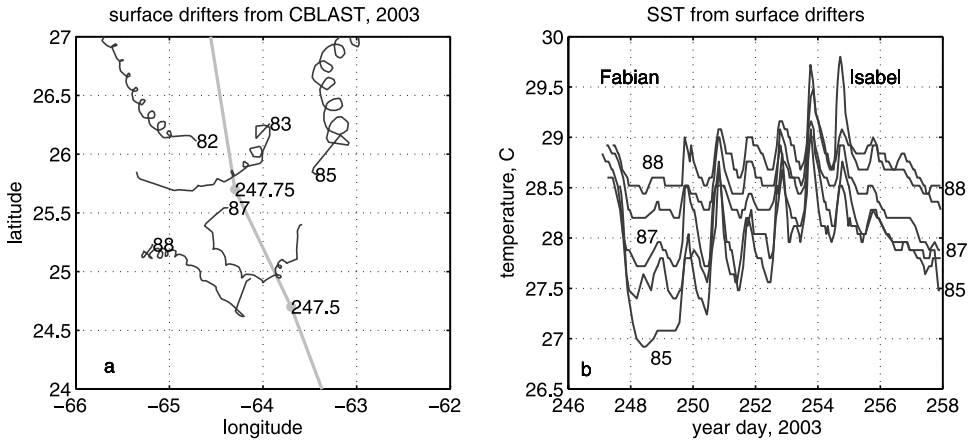


**Figure 4.** (a) The tracks of five satellite-tracked surface drifters launched just ahead of Hurricane Fabian (2003). Six of the eight drifters deployed in the CBLAST pilot study were set in pairs, of which we show only one member. The gray line running south to north is the hurricane track, with year day noted at two points. The numbers 82, 83, etc., are the last two digits of the drifter identifiers, 41582, 41583, etc., that are shown at the starting location of the drifter track. The time shown here spans 11 days. The loops evident in some of the tracks, most notably 85 and 83, are near-inertial period oscillations. (b) Surface temperature reported at roughly 2-hourly intervals by the same drifters shown at left. Hurricane Fabian passed directly over the drifter array near the end of day 247 and caused cooling of about 2.5°C at drifter 85, which was then about 75 km to the right of the track, and much less cooling, about 0.5°C at drifter 88, which was then about an equal distance to the left of the track. Thus the hurricane-induced cooling was monotonically increasing in amplitude from left to right (west to east) across this fairly compact array. Hurricane Isabel passed east to west about 300 km to the south of the drifter array on day 256–257 and caused elevated wind speed beginning on day 255 that suppressed the diurnal cycle and reversed much of the posthurricane warming.

stress that arises from the translation of a vortical wind pattern [*Price*, 1981].

### 2.2.2. Along-Track Variation

[12] There is often a substantial spatial variation of SST cooling in the direction parallel to a hurricane track as well. While this is not directly relevant to the topic of wake warming, we do want to point this out briefly, before we average over it in most of the later analyses. For example, in the Frances case (Figure 3), the SST cooling was greatest in the region around 75°W, where it was approximately 4°C, compared with the CBLAST region centered on 70°W, where the cooling was approximately 2.5°C. On the other hand, the hurricane strength (measured by central pressure) was greatest in the CBLAST region and somewhat reduced farther along the track near 75°W (upper left of Figure 3). Thus the SST cooling and the hurricane strength were evidently inversely related on the largest horizontal scales, O(500 km), seen in these images.

[13] In the CBLAST region, Frances was moving with a fairly steady translation speed, 5 to 6 m $s^{-1}$ and had attained a fairly steady (for a day or so) amplitude, measured by central pressure. Nevertheless, the SST cooling within the CBLAST region varied by roughly 1°C (peak to peak) along a line parallel and to the right of the track, and, e.g., there was a local maximum of cooling at longitude 70°W and a local minimum at longitude 69°W; a typical scale (wavelength) of the SST cooling variability is 25–100 km (but we are not suggesting that there is a peaked spectrum). This kind of smaller-scale, along-track variability of SST cooling can be seen in the wake of most

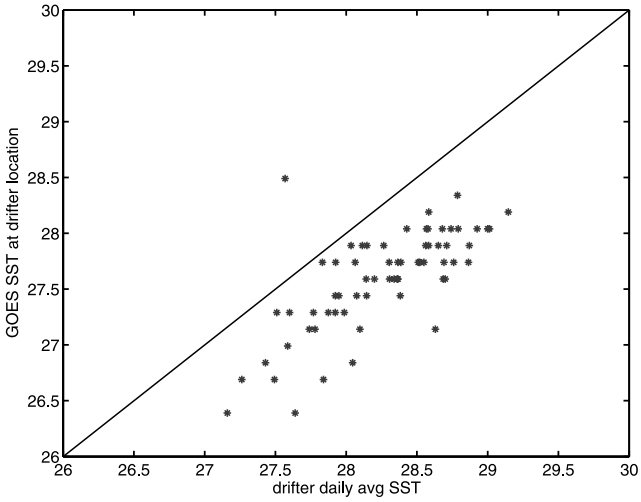


**Figure 5.** GOES-derived SST plotted against the daily average of collocated drifter-observed SST. This small sample from the Fabian case happens to be a useful summary of the GOES data set overall, mostly good but with occasional, localized spurious points, usually along the edge of a cloud mass. The mean offset of GOES data is −0.6°C and the rms difference between GOES and drifter SST is 0.37°C. The latter is closely comparable to the error usually reported for GOES SST retrievals, $2\times$ *rms* = 0.7°C. The one obvious outlier here appears to be an anomalously warm GOES retrieval.

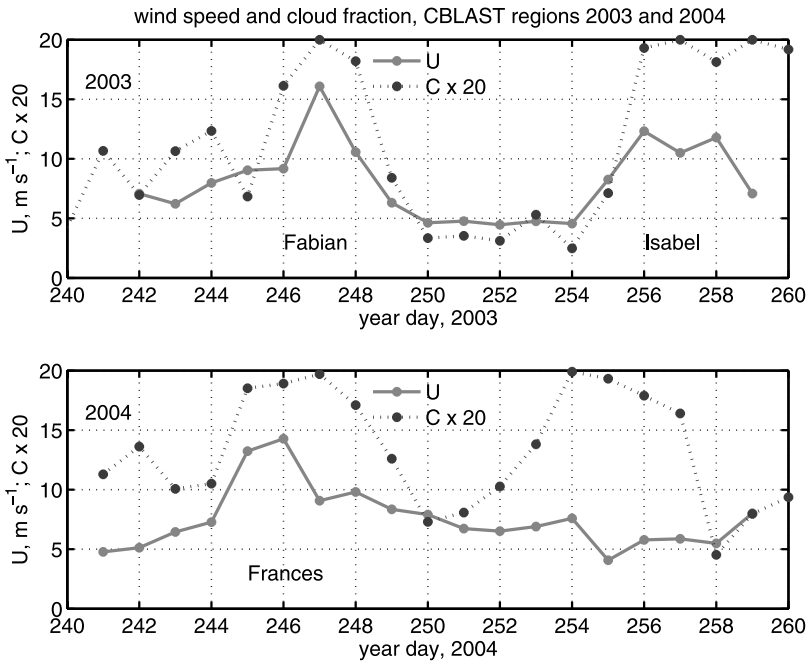


**Figure 6.** Estimates of the spatial mean wind speed from QuikSCAT and of cloud fraction from GOES infrared imagery for the CBLAST regions in (top) 2003 and (bottom) 2004. Note that cloud fraction was multiplied by 20 to fit on the scale appropriate to wind speed. In 2003, the region sampled was centered on Fabian's track at 26°N; in 2004 the region sampled was centered upon Frances' track at 70°W. What is of most relevance here is the wind speed and cloud fraction in the 5-day period following the passage of Fabian (2003) and the 12-day period following Frances (2004).

hurricanes, including Fabian. The source of this along-track variability of cooling is not known, but we suspect that ocean mesoscale variability is one important factor [*Lin et al.*, 2005].

### 2.3. Estimating the Weather

[14] We have already suggested that the wake warming process is mainly local and due to surface fluxes. It follows that posthurricane weather conditions of wind speed and cloud cover are important. To estimate wind speed, we have used QuikSCAT wind retrievals averaged over a region about 4° on a side and centered on the CBLAST regions, Figure 6. The hurricanes appear as strongly muted wind speed maxima having a duration of 1 to 2 days near day 247 in 2003 (Fabian) and by coincidence, on almost the same year day in 2004 (Frances). The maximum wind speed shown here grossly underestimates the maximum winds observed in either hurricane, partly because of the spatial averaging done here and partly because the spatial averaging and geophysical algorithm applied routinely to QuikSCAT are not well-suited to observing the winds of hurricanes. But after the hurricanes pass, the weather conditions were more or less nominal trade winds and well-suited to measurement by QuikSCAT.

[15] After the passage of Hurricane Fabian, the wind speed over the CBLAST 2003 region was steady and light, $U = 5 \pm 0.5$ m s$^{-1}$, for a period of about 5 days, 249–254 (Figure 6, top). Then beginning on day 255 the wind freshened and cloud cover increased markedly as Hurricane Isabel passed about 300 km to the south. Thus the period of fair, trade wind weather over which we will analyze wake warming was brief, only about 5 days, and coincident with a period of rapid wake warming (Figure 4).

[16] After the passage of Hurricane Frances, the weather over the CBLAST 2004 region was somewhat unsettled and defining a period of typical trade wind conditions is not clear cut. Certainly not past day 260, when Hurricane Jeanne passed over the CBLAST 2004 region. If we somewhat arbitrarily choose to analyze wake warming over the intervening 12 days, 248–260, the root mean square wind speed (relevant for estimating wind stress) was $U = 8 \pm 1$ m s$^{-1}$ (Figure 6, bottom). We will argue below (section 4.2.3) that the modest difference in wind speed between these two cases, 5 m s$^{-1}$ versus 8 m s$^{-1}$, which gives a factor 2.5 difference in estimated wind stress, was the main factor that caused the significant difference in warming rates found in these two cases.

[17] Cloud cover can significantly alter the surface heat flux by reducing the incident solar radiation. In the absence of surface radiation measurements, we have attempted to estimate solar radiation beginning with cloud fraction, $C$, estimated from noontime (hourly) GOES infrared images. For the first 5 days post-Fabian, the cloud fraction $C = 0.15$, and then increased dramatically when Hurricane Isabel passed to the south (Figure 6, top). For the 12-day period post-Frances, there was greater cloud cover, averaging $C = 0.7$ but highly variable, $\pm 0.2$, judging from Figure 6, bottom. As we will see in the later analysis, this large

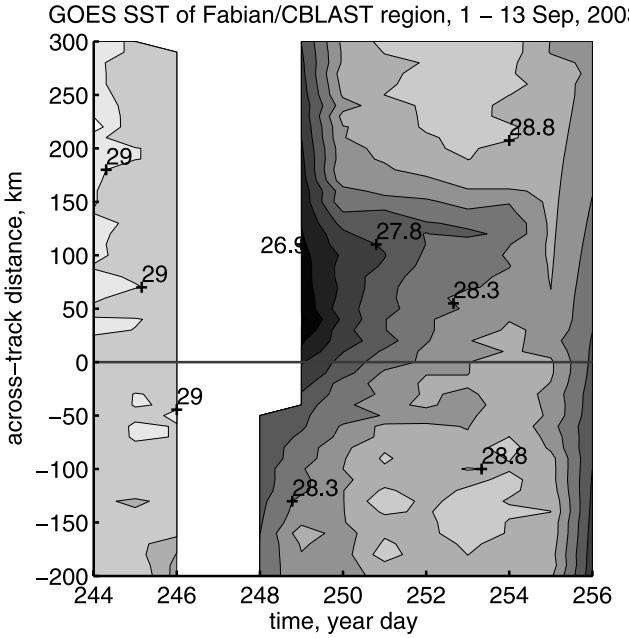


**Figure 7.** GOES-derived SST as a function of distance across the track and time in year days before and after the passage of Hurricane Fabian. This data is an average over about 100 km distance along the track and centered on the CBLAST 2003 field survey region (the rectangle of Figure 2). The cool bias noted in Figure 5 has been removed. The several day gap around day 247 was due to the cloud cover associated with Fabian. The next possible day, 257, was completely obscured by cloud cover from Hurricane Isabel.

variability of cloud cover likely complicates the interpretation of wake warming in the Frances case.

## 3. Wake Warming

### 3.1. Diagnosing the Warming Rate Post-Fabian

[18] A useful understanding of the warming phenomenon starts with an objective estimate of the warming rate. We have done this in two different ways. In the first and most direct way, we have fit a simple function of time to the GOES SST data. The dimensionality of the GOES imagery was first reduced by averaging over a distance of 100 km along the track to yield SST(x, t), Figure 7. We then differenced the prehurricane and the posthurricane data to yield the "cooling," $\delta T(x, t) = SST_0(x) - T(x, t)$. (Note that this is cooling in the usual, temporal sense, which is relevant for hurricane-ocean interaction. In the Frances case coming next we will estimate cooling with respect to the outlying SST and thus cooling in a spatial sense.) For several reasons that will be clear later, we then computed the best fit of an exponential, $\delta T(x, t) = \delta T_0(x) \exp(-t'/\Gamma_f)$, where the amplitude $\delta T_0(x)$ was taken directly from the data, $t'$ is the time elapsed after the hurricane passage, and $\Gamma_f$ is the unknown e-folding time that was to be determined globally, for all $x$ where the cooling was appreciable, $-100 < x < 200$ km. The analysis includes the posthurricane period days 249 through 254, so that the obvious cooling of SST starting on day 255 (Figure 7) has been omitted. As we noted in section 2.3, this 5-day period was characterized by fair weather, light winds, and clear skies.

[19] For the Fabian case, this best-fit e-folding time was found to be $\Gamma_f = 4.5 \pm 1$ days, where the subscript $f$ refers to fitting (a differential estimate of $\Gamma$ is coming next). An exponential gives a plausible fit to the data, with the best fit accounting for more than 95% of the variance of the observed cooling. The uncertainty is estimated from the half-width of the misfit, i.e., $\Gamma_f = 5.5$ days gives twice the minimum misfit.

[20] Two remarks regarding the procedure and it's description. First, we often speak of "warming rate," for which the most convenient quantitative measure is the inverse of the normalized warming rate, $\Gamma = (\frac{-1}{\delta T}\frac{d\delta T}{dt})^{-1}$, the e-folding time reported in days. This single number appears to be a useful characterization of the entire (5 day) data set. On the other hand, as we will see next, the absolute warming rate, $\frac{d\delta T}{dt}$, depends upon the amplitude of the cooling and thus varies with both the spatial position and time. Second, by estimating the cooling with respect to the prehurricane SST, it is implicit that the SST was warming back toward the prehurricane value. This seems plausible in this case but is not guaranteed.

[21] A second and in some ways more insightful way to view the warming rate is as a function of the cooling amplitude. The rate of change of SST was computed by first differencing the daily composite GOES images (the smaller points of Figure 8) and the corresponding daily averages of drifter-measured SST (the larger open dots of Figure 8) and then plotted against the daily average cooling. Any process that causes SST to vary at a point in space will contribute variance to the first time derivative made from the GOES satellite-derived SST, e.g., horizontal advection or outright noise in GOES-derived SST, and hence it is not unexpected that there is a fair degree of scatter in the satellite-derived estimates of warming rate. However, the variability within the surface drifter-derived estimates is comparable, suggesting that the apparent scatter seen here was mainly geophysical rather than instrumental and was not due primarily to horizontal advection, which is presumably small in the drifter SST. Note that the surface drifters showed rapid cooling from the first hour of their deployment, which was about a day in advance of the hurricane passage. Thus when we estimate the cooling from these drifter data we do so with respect to a bias-adjusted, prehurricane, spatial average of the GOES data, $\delta T = SST_0 - T$, where $SST_0 = 29.3°C$.

[22] There was a significant positive correlation of warming rate and cooling amplitude, i.e., the coolest part of the wake (region around $x \approx 70$ km) warmed the fastest in an absolute sense, which is evident also by inspection of the satellite images. A line $\frac{d\delta T}{dt} = a_1\,\delta T + a_0$ was least-squares fitted to the resulting collection of points, giving equal weight to satellite-derived and drifter-derived data. The intercept $a_0 \approx 0$, suggesting that the cooling amplitude as computed here is indeed the relevant, physical temperature difference in so far as the rate of warming is concerned. The slope of the line, $a_1 = -0.177\ d^{-1}$, makes an estimate of the ensemble-averaged (all of the drifter and relevant GOES data) normalized rate of warming, $\frac{-1}{\delta T}\frac{d\delta T}{dt} = a_1$, and the (negative) inverse slope is an e-folding time $\Gamma_d = -a_1^{-1} = 6.0 \pm 0.5$ days. The subscript $d$ refers to an estimate of $\Gamma$

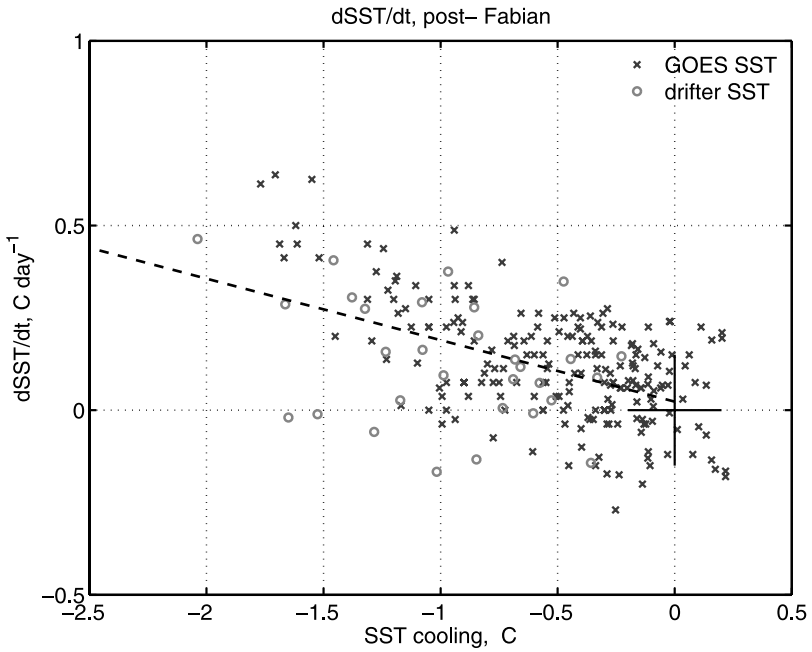


**Figure 8.** The warming rate computed by first differencing GOES SST daily composite images (the small cross) and by first differencing the daily averaged drifter SST (larger open points). These data are from the posthurricane time interval days 249 through 254 that were fair, trade wind weather. The cooling of SST that starts on day 255 and that we have attributed to Hurricane Isabel has thus been omitted from this analysis. The dashed line is a linear fit whose inverse slope gives an estimate of the ensemble-averaged e-folding time, $\Gamma_d = 6 \pm 0.5$ days.

made on differentiated data. The uncertainty noted here is the standard error of the slope. This second estimate of the e-folding time is just barely consistent with the estimate $\Gamma_f$ made by fitting to the SST surface noted above. When we cite a single value of the e-folding time we will use a rounded average, $\Gamma = 5 \pm 1.5$ days, with an uncertainty that spans both estimates.

### 3.2. Diagnosing the Warming Rate Post-Frances

[23] The Frances case differed from the Fabian case with respect to the post-hurricane weather conditions and regards the extent and kind of available data. In place of the fair, clear weather that occurred for at least a short period post-Fabian, the weather post-Fabian was unsettled. Much of this was hurricane-related, e.g., the significant increase in cloud cover on day 254 was associated with the passage of Hurricane Ivan through the Caribbean Sea, though with little apparent increase in wind speed in the CBLAST region. The result was that clouds obscured any specific point on the sea surface from GOES infrared imaging (Figure 3) on roughly half of the relevant days post-Frances (before the arrival of Hurricane Jeanne on day 261). (After the analysis for this study had been largely completed we became aware of the microwave sounder (TRMM Microwave Imager, or TMI) SST analysis available at the Remote Sensing Systems Web site, http://www.ssmi.com/. The TMI-derived SST analysis largely eliminates the obscuring effects of cloud cover on infrared imagery [*Wentz et al.*, 2000], but at the expense of some temporal and spatial resolution compared with GOES. We have compared a TMI-derived SST data set with the GOES imagery shown here and find the two data sets to be similar overall, though the TMI-derived SST data is smoother spatially and in time, and has far fewer spurious retrievals.) While warming of the cool wake is clearly evident in the GOES images, nevertheless, the discontinuous GOES record makes the previous analysis of the warming rate problematic.

[24] To diagnose the wake warming in this case we have relied instead upon the 25-strong surface drifter data set, Figure 9. The drifter array was large enough that the drifters farthest from or to the left of the track (drifter 41938 at x = −34 km and drifter 41926 at x = 170 km) showed very little cooling due to the passage of Frances, $|\delta T| \leq 1$°C in many drifter records (Figure 10 and see *D'Asaro et al.* [2007] for much more detail on the SST cooling due to Frances). Notice that there was little or no posthurricane warming of SST evident at the two outlying drifters, 41926 and 41938; the SST cooled from about 29.5°C to about 28.7°C during the hurricane passage and then remained nearly constant for the following several weeks. Satellite imagery indicates the same thing. Hence, the cooling in this case is computed with respect to the (spatially) outlying SST, i.e., $\delta T = SST_0 - T$ where $SST_0 = 28.7$°C, by inspection of these data. In effect, we are assuming that SST in the wake of Frances would have warmed to 28.7°C, given sufficient time and steady weather conditions, and not to the slightly warmer prehurricane SST, about 29.5°C.

[25] The ensemble-averaged, least squares fit of an exponential to the collection of 25 drifters that were within 200 km of the CBLAST region (Figure 9) and over the period 248–260 indicates an e-folding time $\Gamma_f = 20 \pm 10$ days, where the uncertainty cited here is an average of a somewhat

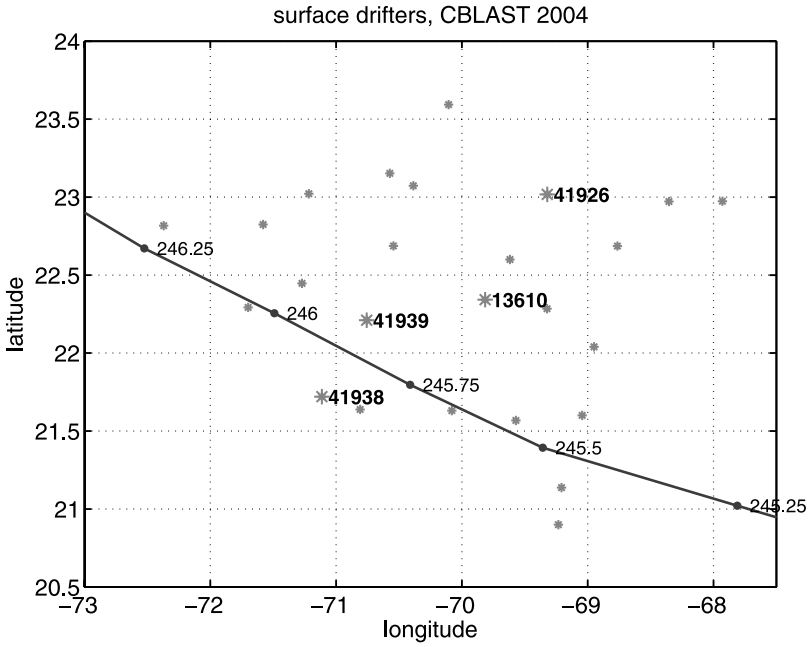


**Figure 9.** Positions of 25 surface drifters that were within about 200 km of the CBLAST 2004 central region on day 245.7. SST from the four drifters shown with five digit identifiers are shown in the next figure.

asymmetric misfit, 15 days to about 45 days. The best fit accounts for about 90% of the variance of $\delta T$, which would appear to be a large fraction. Nevertheless there were several drifter records for which this exponential is not a good characterization, e.g., drifter 41939 of Figure 10.

[26] The warming rate computed by first differencing the daily averages of drifter SST (Figure 11) appears to be almost random, despite that GOES images and the drifter data as a whole show an unmistakable though gradual warming over the two week period following Frances

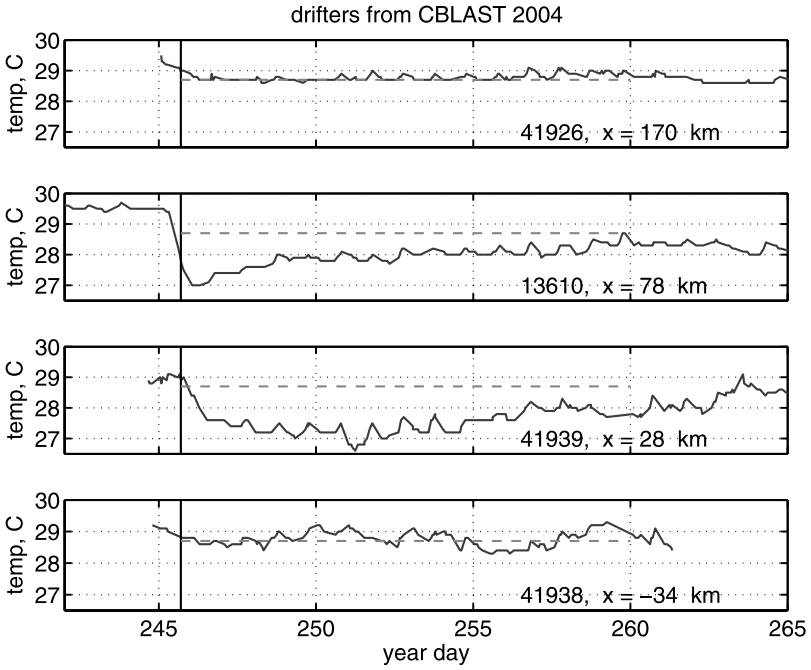


**Figure 10.** SST measured by four surface drifters that spanned the track of Hurricane Frances (see the previous figure for positions). The drifter identifier is at lower right; drifter 13610 was part of an operational deployment, while the other three drifters were air-launched just a day ahead of Hurricane Frances. The across-track distance to the hurricane track is shown at lower right of each panel; distance to the left of the track is negative, distance to the right is positive. The nearest approach in time of Hurricane Frances is noted by the vertical line at year day = 245.7. The dashed line at T = 28.7°C is the outlying SST used as the reference when computing "cooling" in this case.

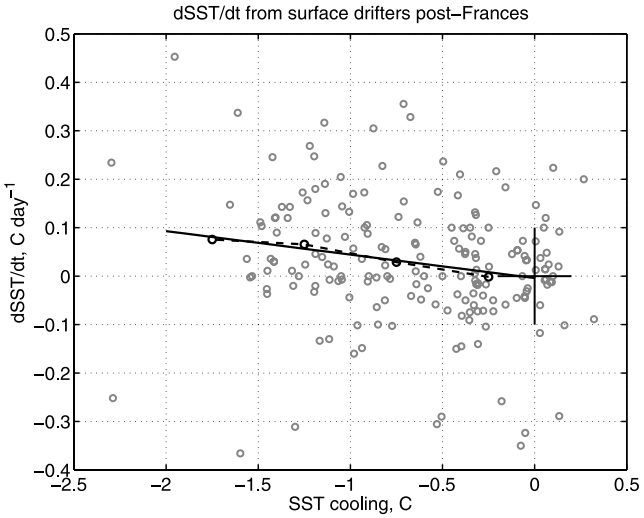


**Figure 11.** The time rate of change of daily averaged, drifter measured SST shown as a function of cooling, $\delta T = T - 28.7$. There is a weak correlation between positive rate of change of SST and cooling magnitude. A binned average over cooling intervals of 0.5°C is shown by the dashed, broken line. A linear fit is the straight line whose inverse slope indicates an e-folding time scale $\Gamma_d = 20 \pm 8$ days.

(Figure 3). The large, day-to-day, random (from this ensemble-average perspective) variation of SST nearly swamps the wake warming signal, which does, however, appear upon bin-averaging over intervals of 0.5°C (the dashed broken line of Figure 11) or by making a linear fit (the thin line). Either averaging method indicates a weak, positive correlation between warming rate and cooling amplitude, and the inverse slope of the linear fit gives an e-folding time $\Gamma_d = 20 \pm 8$ days, which is consistent with $\Gamma_f$ noted above and also substantially uncertain. This is evidently a more complex example of wake warming than was found post-Fabian, due probably to the unsettled weather following Hurricane Frances and to the somewhat greater spatial extent of the drifter data set (more on this below). What we can say with some confidence is that the e-folding time of this cool wake was considerably greater, by roughly a factor of three to five, than was found in the Fabian case.

[27] Notice that as in the Fabian drifter-measured SST data, there was an obvious diurnal cycle of SST, occasionally as large as 0.5°C, but quite variable from day-to-day. The ensemble average amplitude of the diurnal cycle was $\langle T' \rangle = 0.19$°C, which is only about one third of the ensemble average value estimated from the Fabian data set. As we will argue in section 4.3, the generally smaller amplitude of the diurnal cycle in this case is consistent with the slower rate of wake warming found here, and, along with other properties of the warming, leads to the inference that the wake warming process is driven mainly by surface heat fluxes and wind. The standard deviation of $T'$ was 0.17°C, which is comparable to the mean. This large standard deviation of the diurnal cycle amplitude indicates significant day-to-day variation in either or both the cloud cover and the wind speed.

[28] The Frances drifter data set is large enough both in spatial extent and in the number of drifters that it is possible to look within the data set for some of the quantities that we have otherwise represented by an ensemble average. The amplitude of the wake warming and the e-folding time may be estimated for each drifter by fitting $\delta T_i = \delta T_{0i} \exp - t/\Gamma_i$, where the subscript $i$ refers to a specific drifter. This reveals that the e-folding time $\Gamma_i$ at a given drifter varied over a range from about 10 days to about 35 days, for those drifters that showed a significant cooling, $\geq 1$°C ($\Gamma$ is poorly defined on drifter SST records like that of drifter 41926, Figure 10, that showed almost no cooling). The shorter e-folding times were found mainly on the northwestern side of the drifter array, where cooling was greater than average, and the longer e-folding times found mainly on the southeast side, where cooling was somewhat less than average. The diurnal cycle amplitude may also be computed over each individual drifter, and when we compare the diurnal cycle amplitude with the wake warming amplitude divided by the folding time, i.e., $\delta T_{0i}/\Gamma_i$, (Figure 12) we find a coherent variation of wake warming and diurnal warming. For now we are going to draw only the broadest conclusions: First, that at least a portion of what looks to be noise in the ensemble statistics of the Frances case, Figure 12, is likely due to spatial variation of cloud cover and wind over the drifter array. Second, the wake warming rate was largest on the drifters (and thus in space) where the diurnal cycle amplitude of SST was also largest. This is additional evidence (beyond the comparison with the Fabian case noted above) that wake warming and the diurnal cycle are closely related phenomena, something we will follow up in the next section.

### 3.3. Summary and Inferences From the Observations

#### 3.3.1. Wake Warming Process

[29] Four qualitative properties of the SST warming gleaned from this analysis suggest that the wake warming process is mainly local (i.e., that it does but not depend significantly upon horizontal variation in the ocean) and that

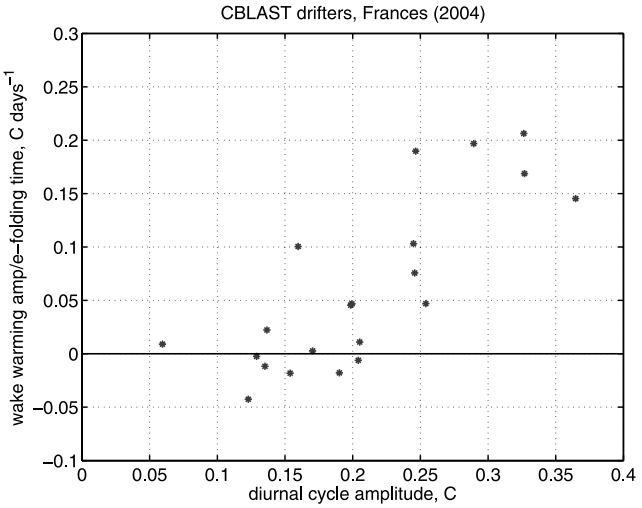


**Figure 12.** On a given CBLAST (2004) drifter; the drifter-average diurnal cycle amplitude and the wake warming amplitude divided by the e-folding time at that drifter, $\delta T_{0i}/\Gamma_i$. This analysis is for the posthurricane period 248–260 and omits four drifters that showed no appreciable cooling, e.g., 41926.

it is driven by surface heat fluxes. The first of these properties is that the SST cooling faded away while remaining more or less fixed in space horizontally (though there are occasions when pattern translation and stirring is also evident in satellite imagery and expected given the low-frequency drifter displacements, Figure 4a). Second, wake warming was most rapid where cooling was largest, in the center of a wake, rather than on the edges, as would be the case if it was due mainly to small-scale, horizontal mixing, for example. Third, the spatial integral of cooling clearly decreased in time, so that something more than a conservative mixing or stirring process must be involved in the warming process. Fourth, we found that wake warming was most rapid during periods of light wind and clear skies (the rapid warming in the Fabian case) and that the rate of wake warming covaries with the amplitude of the diurnal cycle of SST, as just noted in the Frances analysis.

#### 3.3.2. Warming in These Two Cases

[30] Our intent in this paper is to emphasize the process of wake warming that occurs during more or less homogeneous, trade wind weather. Such fair weather often does follow a hurricane, but during the very active 2003 and 2004 hurricane season in the western North Atlantic, hurricanes followed one another so closely that the duration of fair, trade wind weather following a given hurricane was brief, only about 5 days post-Fabian and 12 days post-Frances (and then we have to allow in the heavy cloud cover due to Hurricane Ivan). Wake warming may be reversed by a moderate increase in wind speed, as noted in the Fabian case. These two cases make clear that the warming of a hurricane's cool wake is not necessarily monotonic in time, and just as well, wake warming may not proceed all the way back to the prehurricane value before the onset of another weather event. Even within a period of nominal, trade wind weather, the warming rate can vary considerably from case to case; post-Fabian, we estimate that the e-folding time of the cool wake was 5 ± 1.5 days, while post-Frances, we infer an e-folding time of 20 ± 10 days, or greater by a factor of about three to five.

## 4. Simulations and Scale Analysis of the Wake Warming Process

### 4.1. Numerical Experiments

[31] To make a start toward understanding the dynamics of the wake warming process, we have run several experiments with a one dimensional upper ocean model [*Price et al.*, 1986; hereinafter referred to as PWP] under prescribed atmospheric conditions, i.e., one-way interactive. We are not aware of anything that makes this upper ocean model uniquely suited for this purpose and expect that other models would give more or less similar results. A detailed simulation of upper ocean properties and SST would require hourly or better resolution of surface heat fluxes and wind stress. The atmospheric and radiation flux measurements required for this resolution are not available in the post-hurricane periods of interest here. Instead, we will attempt to construct a coarse-grained estimate of the surface fluxes that will nevertheless acknowledge one important aspect of air-sea interaction, namely, that the surface heat flux varies diurnally in most fair weather conditions.

[32] A small number of dropsondes deployed around the periphery of Hurricane Frances indicated Tair = 28°C and relative humidity = 80%. These are near climatological values for this region and season [*Bunker*, 1976, Figure 10] and hence we will assume these values throughout. These air temperatures are potentially important variables, and we will later note briefly what this assumption entails. Solar insolation was computed from the year day and latitude and assuming a nominal atmospheric transmission and sea surface albedo; in the absence of cloud cover, the noon maximum solar insolation was estimated at about 1050 W $m^{-2}$. The simplest parameterization of cloud effect on solar insolation, a factor $(1-0.7C)$, was then applied, with cloud fraction taken from the satellite-derived data of section 2.3. In the first experiment we will use a nominal value of cloud cover, C = 0.4, that is a rough characterization of the cloud cover over the CBLAST regions prior to the hurricanes (Figure 6). Wind stress was computed from the observed, estimated wind speed, $U_{10}$ = 6 m $s^{-1}$ using the neutral drag coefficient of *Fairall et al.* [2003], roughly $C_d = 1.1 \times 10^{-3}$.

[33] The ocean model was integrated ahead until SST came into a near equilibrium at about 29.8°C, which is just slightly warmer than the observed, prehurricane SST in either case. This equilibrium SST is determined by the prescribed atmospheric conditions, together with the flux parameterizations. Given this fair, trade wind weather, there was a large amplitude diurnal cycle in the surface heat flux and within the upper ocean (Figure 13); the net heat flux was significantly positive (warming) during the middle of the day, and the upper ocean became stably stratified as SST warmed by about 0.5°C in the early afternoon. During the evening, the surface heat flux was negative, or cooling, and sufficient to extract the heat (enthalpy) stored during the previous half day. When the SST was at the equilibrium value noted above, the net heat flux summed over a day was nearly zero, and the upper ocean diurnal cycle was closed, or repeating.

[34] A very strong, ad hoc wind was then imposed for half a day, with the result being strong vertical mixing within the upper ocean that cooled SST by about 3°C. Once this wind event had ceased, the weather was presumed to return to the nominal trade wind conditions noted above. Because the SST had been reduced below the equilibrium value, the heat loss (the sum of sensible, latent, and net long wave radiation) was also reduced in magnitude from roughly $-250$ W $m^{-2}$ in the prewind event equilibrium state, to about $-100$ W $m^{-2}$ just after the mixing event (Figure 13a). Since the solar insolation was unchanged, there was then a net (daily averaged) surface heat flux given by the difference between the prewind and postwind mixing event heat loss, $\delta Q \approx 150$ W $m^{-2}$, which was positive (warming) since the SST anomaly was cooling. This positive heat flux anomaly caused the upper ocean to begin to warm, and if the model had been run long enough, roughly a month plus (while suppressing the seasonal variation of solar insolation), the SST would have returned closely to the equilibrium SST for these weather conditions, 29.8°C.

[35] As we noted above, the equilibrium SST is determined by the prescribed atmospheric conditions; however, the time required for SST to return to equilibrium, i.e., the relaxation time or e-folding time of the cool SST anomaly, is

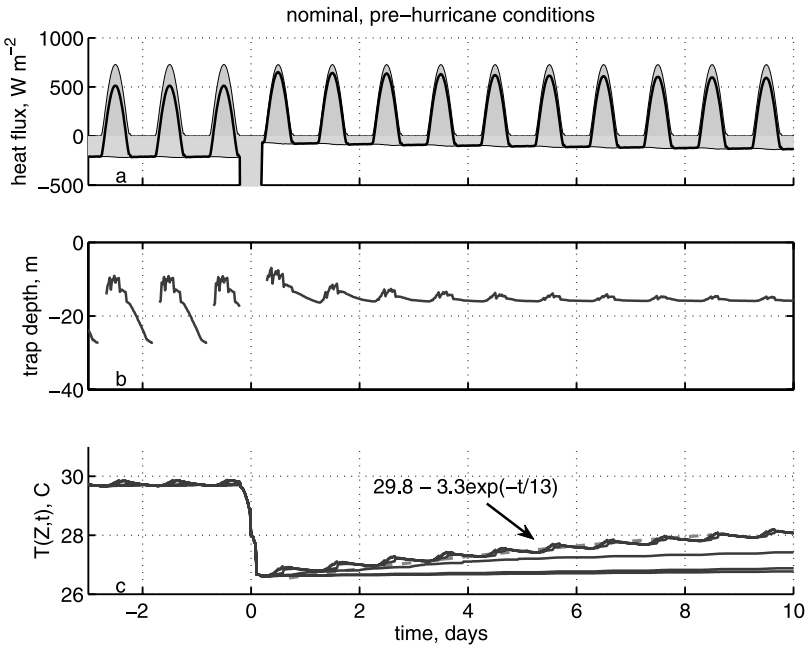


**Figure 13.** A simulation by a one-dimensional upper ocean model showing a trade wind regime with cloud cover and wind speed taken from prehurricane conditions and perturbed by a strong, transient wind event around time = 0. (a) The surface heat fluxes: solar insolation (light grey), heat loss (dark grey) and the net heat flux (black line). (b) The trapping depth, $D$, of the surface layer defined by (1). (c) Ocean temperature at depths of 0 (SST), 5, . . .25 m. Note that the wind event caused SST to cool by about 3°C. After the wind event, the SST and near-surface layer then began to warm back toward the equilibrium SST, about 29.8°C. The postwind event cooling can be characterized as a decaying exponential with an e-folding time of about 13 days (the dashed line). The gradual warming at depths of 20 m and below was due to penetrating solar radiation.

determined by the thickness of the upper ocean layer that absorbs the anomalous heat flux. This thickness is dependent upon upper ocean dynamics and the surface fluxes. An integral measure of the surface layer thickness is the so-called trapping depth [PWP],

$$D = \frac{1}{\Delta T(0)} \int_{z_r}^{0} \Delta T(z) dz \qquad (1)$$

where $z_r$ is a deep level that is almost unaffected by warming, $z_r = 40$ m and $\Delta T(z) = T(z) - T(z_r)$ is the warming with respect to $T(z_r)$. During the post wind-event period, $D \approx 15$ m (Figure 13b) in this simulation. For these nominal trade-wind conditions the time-dependence of the SST cooling can be characterized as an exponential decay with an e-folding timescale of about 13 days (the dashed line of Figure 13c).

[36] In a second and a third experiment we started with the same initial conditions and applied the same intense wind event. After the wind event, the wind speed and cloud cover were set to the values that were estimated post-Fabian, wind speed $U = 5$ m s$^{-1}$ and cloud fraction C = 0.15, and then in the third experiment, with the values estimated post-Frances, $U = 8$ m s$^{-1}$ and C = 0.7 (section 2.3). The ocean response was qualitatively similar in that there was again a more or less exponential return of SST toward an equilibrium, but with two quantitative differences. First, the equilibrium SST was somewhat different, approximately 30.3°C and about 28°C for the post-Fabian and post-Frances conditions, respectively (the simulated SST does not reach this post wind event equilibrium in the 10 day period shown here). Second, the e-folding time of the cool anomaly was markedly different in these two experiments, about 7 days for post-Fabian conditions and much longer, about 24 days for post-Frances conditions. These are roughly consistent with the observed e-folding times (section 3.1 and 3.2). However, there is some discrepancy in the amplitude of the wake warming in the Frances case; the equilibrium SST in the numerical experiment was 28°C, while a somewhat warmer value, 28.7°C, was inferred from the drifter data set (section 3.2). The difference, 0.7°C, is a significant fraction of the cooling, about 2°C, and the sense of the difference is that the absolute warming rate in the Frances experiment was somewhat less than observed in the surface drifter data, though the e-folding times are roughly comparable.

[37] In all, these numerical experiments appear to support the inference from observations that the wake warming process is mainly local (depth- and time-dependent) and driven by surface fluxes. There is no doubt that the e-folding time found in the numerical experiments is sensitive to posthurricane weather conditions.

### 4.2. A Scale Analysis of Wake Warming

[38] Our goal is not primarily to make a detailed simulation SST (if for no other reason than the lack of adequate atmospheric data) but rather to develop an understanding of

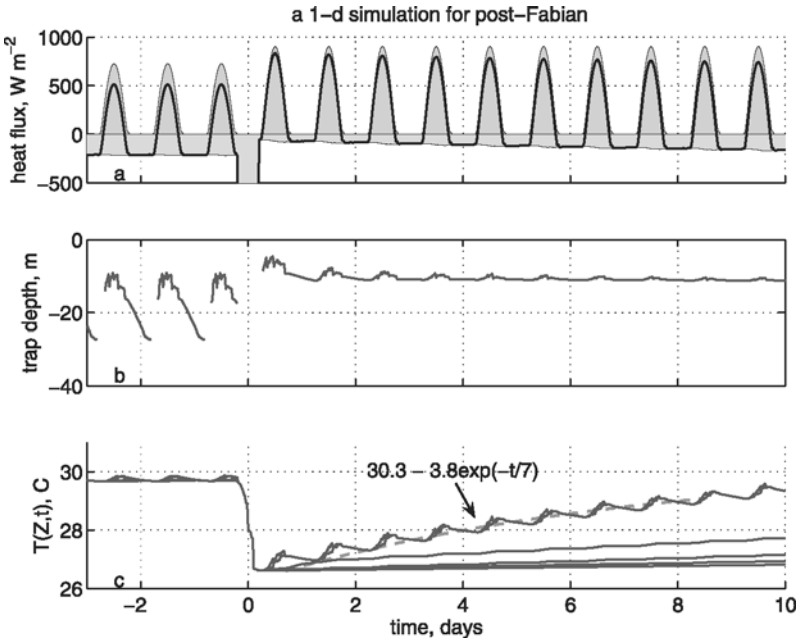


**Figure 14.** A simulation by a one-dimensional upper ocean model showing a trade wind regime with cloud cover and wind speed taken from prehurricane conditions and perturbed by a strong, transient wind event around time = 0. After the wind event, the weather conditions were prescribed to match post-Fabian conditions. (a) The surface heat fluxes: solar insolation (light grey), heat loss (dark grey), and the net heat flux (black line). (b) The trapping depth of the surface layer. (c) Ocean temperature at depths of 0 (SST), 5, . . .25 m. After the wind event, the SST and near-surface layer began to warm back toward the equilibrium SST, about 30.3°C in this case. The postwind event cooling can be characterized as a decaying exponential with an e-folding time of about 7 days (the dashed line).

the physical dynamics of the warming process. As a test, can we offer a plausible, semiquantitative explanation of the very different e-folding times found in the Fabian and Frances cases?

[39] The numerical experiments suggest that the posthurricane SST evolution might be understood by analyzing the heat budget of an upper ocean surface layer

$$\frac{d\ \delta T}{dt} = \frac{\delta Q}{\rho C_p D}, \tag{2}$$

where $\rho$ and $C_p$ are the constant, nominal density and heat capacity of sea water. The task is then to estimate (or model) the relevant heat flux, $\delta Q$, and just as importantly, the surface layer thickness, $D$, the so-called trapping depth, which varies by a factor of about three from the Fabian case to the Frances case, cf. Figures 14b and 15b.

#### 4.2.1. Heat Flux Anomaly

[40] The heat flux anomaly $\delta Q$ is presumed to result from an SST cooling-induced shift away from a balance between heat gain due to solar insolation, $Q_{sol}$, and heat loss due to the sum of sensible, latent and infrared heat fluxes, $Q_{loss}$, i.e., at the the equilibrium SST, $Q = Q_{sol} + Q_{loss} = 0$, averaged over a day. $Q_{sol}$ is presumably unaffected by SST, while $Q_{loss}$ can be significantly reduced in magnitude by cooling of SST (assuming air temperatures are constant). In the range of SST and wind and air temperatures that are characteristic of the late summer trade wind regime (SST = 29°C, $T_{air}$ = 28°C, relative humidity = 80% and wind speed = 3–9 m s$^{-1}$ [*Bunker*, 1976, Figure 10]) the heat loss from the sea surface estimated by bulk formulae varies with SST roughly as $\partial Q_{loss}/\partial SST = \lambda = -65$ W m$^{-2}$ C$^{-1}$ (Figure 16). Of this, about 80% is due to reduction of the latent flux, about 15% is due to a decrease of the sensible heat flux and a very small contribution comes from a decrease of net long wave radiation. The heat flux anomaly for these nominal trade wind conditions may then be estimated approximately by

$$\delta Q = \lambda \delta T, \tag{3}$$

where $\delta T$ is the cooling amplitude computed with respect to the equilibrium SST. Judging from Figure 16 the coefficient $\lambda$ varies by up to ±50% over the extremes of wind speed and SST range shown here, but for the purpose of a scale analysis we are going to take $\lambda$ to be the constant noted; (3) then amounts to a linearization of $Q_{loss}$ (SST).

[41] The temperature difference $\delta T$ of (3) is with respect to the equilibrium SST at which the net heat flux would presumably vanish. This is not directly observable in field data and has to be inferred. In the Fabian case it seemed plausible to assume that the posthurricane equilibrium SST would be the prehurricane value, 29.3°C, and which is likely to give a reasonable estimate for most early or midseason hurricanes. However, in the Frances case, it seemed evident that SST within the cool wake was not going to warm beyond the SST of the outlying sea surface, which was quasi-steady at approximately 28.7°C, and which we therefore took as the equilibrium SST.

[42] As we will see below, this linearization of the heat flux via (3) leads to exponential time dependence of a cool

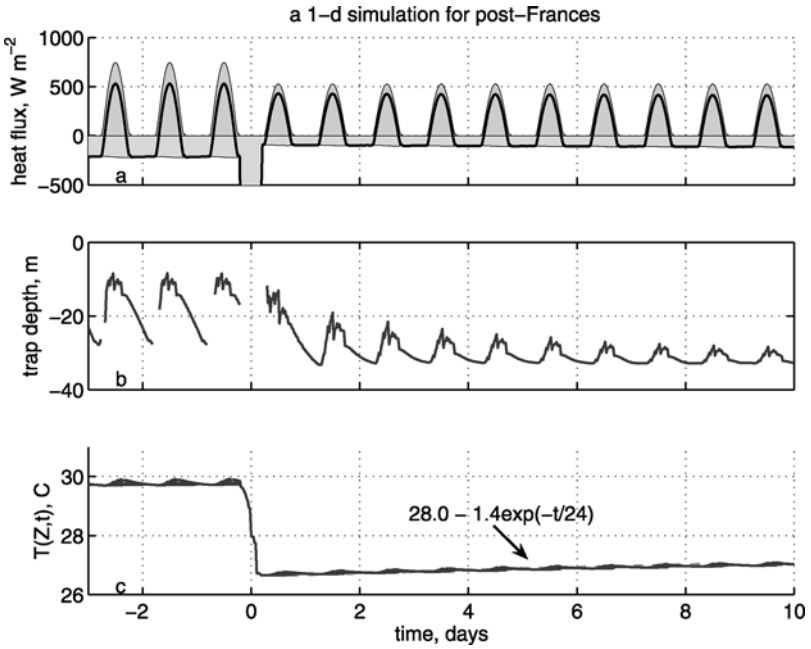


**Figure 15.** A simulation by a one-dimensional model with a trade wind regime perturbed by a strong wind event around time = 0. The post wind event conditions were prescribed to match post-Frances conditions. (a) The surface heat fluxes: solar insolation (light grey), heat loss (dark grey), and the net heat flux (black line). (b) The trapping depth of the surface layer. (c) Ocean temperature at depths 0 (SST), 5, . . .25 m. The wind event around t = 0 caused SST cooling of about 3°C. The SST and near-surface layer (depths < D) then began to warm back toward the equilibrium SST, about 28.0°C, with an e-folding time of about 24 days (the dashed line).

SST anomaly and so is a very useful idealization or approximation. However, if adequate atmospheric data were available, then the approximations inherent in (3) could be bypassed, or at least, verified.

#### 4.2.2. Trapping Depth

[43] Under the conditions of fair weather and strong solar heating that often prevail over a cool wake, the warming and stabilizing heat flux anomaly $\delta Q$ is evidently absorbed within a rather thin surface layer of thickness, $D \approx 10-30$ m, judging by Figures 14 and 15. This depth appears to be set by the process of diurnal cycling; the warm diurnal layer that formed just after the wind event was not completely erased the following evening and was reinforced on each of the following days (Figure 17). Thus a shallow thermocline was formed on a depth scale that was set by the diurnal cycle.

[44] An important modeling assumption is that the appropriate $D$ can be estimated by the scale analysis of the trapping depth of the diurnal cycle [PWP, equation (16)],

$$D \frac{\tau P_f/\rho}{\sqrt{Q * P_Q}}, \tag{4}$$

where $P_f = (1/f)\sqrt{2-2\cos(fP_Q)}$ with $f$ the Coriolis parameter, and $P_Q$ is half the duration of positive heat flux, roughly 6 h. The buoyancy flux

$$Q* = Q_n g\alpha/(\rho^2 C_p)$$

is proportional to the noon (maximum) heat flux, $Q_n$, and $\alpha = -\partial\rho/\partial T \approx 0.3$ kg m$^{-3}$ C$^{-1}$ is (negative) the thermal expansion coefficient for sea water at warm temperatures

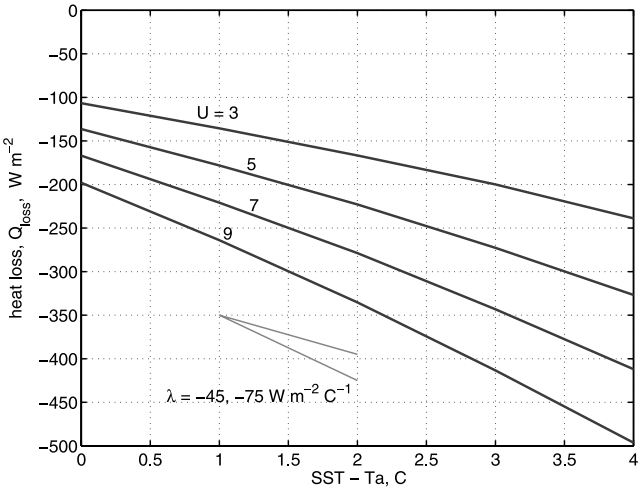


**Figure 16.** The heat loss from the ocean to the atmosphere (the sum of latent, sensible, and net infrared heat fluxes) estimated from standard bulk formula for typical late summer trade wind conditions and for wind speeds of 3, 5, 7, and 9 m s$^{-1}$ (the four curves). For the purpose of estimating the anomalous heat flux due to hurricane-induced SST cooling we require the derivative, $\lambda = \partial Q_{loss}/\partial SST$, which varies with the wind speed and the air-sea temperature difference. For a nominal wind speed, 7 m s$^{-1}$, and air-sea temperature difference, SST − Ta = 2 C, $\lambda \approx -65$ W m$^{-2}$ C$^{-1}$.

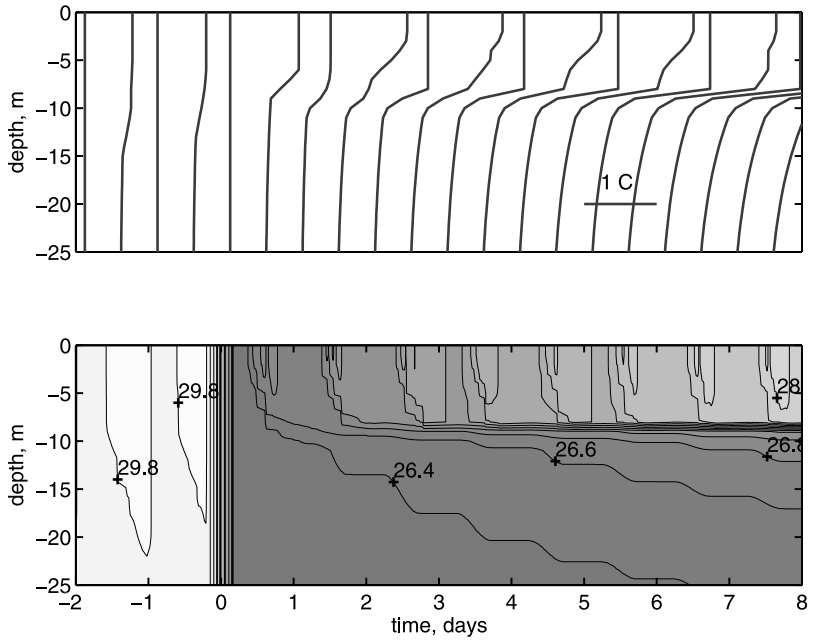


**Figure 17.** Temperature in the upper 25 m of the Fabian experiment. (top) Temperature profiles plotted every 12 h. The deepest temperature corresponds with the timescale below. (bottom) Temperature contours at 0.2°C interval. Note that after the wind event, a transient thermocline forms at a depth of about 10 m, the trapping depth in this experiment, cf. Figure 14b.

and $g$ is the acceleration of gravity. At latitudes not too far from the equator, the timescale $P_f$ can be approximated well enough by $P_Q$ and then

$$D = C_D \frac{\tau/\rho}{\sqrt{Q*/P_Q}}. \tag{5}$$

To be sure, we expected that the $D$ of (4) might be proportional and approximately numerically equal to the trapping depth required by (2). Comparisons with numerical solutions indicated the similarity constant $C_D = 1.2$ (not to be confused with the drag coefficient, $C_d$).

[45] For typical summer trade wind weather conditions of light wind and strong solar insolation, the $D$ estimated by (5) will be rather thin, 10–30 m. $D$ will also be quite variable from day to day if, as is usually the case, the wind or cloud cover is variable from day to day. In this analysis, however, we are attempting to characterize the diurnal cycle by averaged values of the surface fluxes, as if the diurnal cycling was homogeneous (as in the numerical experiments).

#### 4.2.3. Parameter Dependence of the e-Folding Timescale

[46] Substituting the heat flux anomaly (3) and the estimate of $D$ given by (5) into the surface layer heat budget (2) gives

$$\frac{d\ \delta T}{dt} = \frac{\delta Q}{\rho C_p D} = \frac{\lambda \delta T \sqrt{Q_n/P_Q}}{C_D C_p \tau} = \frac{\lambda \delta T \sqrt{Q_n}}{C_D \tau} \sqrt{\frac{g\alpha}{P_Q \rho^2 C_p^3}}. \tag{6}$$

The solution for the SST anomaly is then an exponential decay,

$$\delta T = \delta T_0 \exp(-t/\Gamma), \tag{7}$$

where the e-folding time is

$$\Gamma = c \frac{\tau}{\lambda \sqrt{Q_n}}, \tag{8}$$

and $c$ is the product of the similarity constant, $C_D$, and known physical constants,

$$c = \frac{C_D \rho C_p^{3/2}}{\sqrt{g\alpha/P_Q}} = 2.7 \times 10^{10}\ \mathrm{kg}^{1/2}\ \mathrm{ms}^{-3/2}\ \mathrm{C}^{-1},$$

for the cases at hand. Exponential time dependence follows from the assumption that the heat flux anomaly is proportional to the SST anomaly and that the depth scale $D$ is set mainly by something else, namely, the externally imposed wind stress and the noon maximum heat flux, $Q_n$ (which is dominated by solar insolation but is weakly dependent upon $Q_{loss}$ and thus upon $\delta T$, Figure 14a and 15a). Note that this solution for e-folding time is sensitive to wind speed, increasing roughly as wind speed squared (Figure 18). The e-folding time is proportional to $\lambda^{-1}$, and is rather insensitive to the noon maximum heat flux, increasing as $Q_n^{-1/2}$.

[47] The e-folding time given by (8) can be regarded as an approximate solution of the PWP upper ocean model under rather idealized (though fairly common) conditions, namely steady wind stress and homogeneous but diurnally varying heat fluxes. From comparisons of (8) with numerical solutions over a wide range of $Q_n$ and $\tau$ (Figure 18), we find that the scale analysis replays the numerical model result reasonably well for all but the lowest wind speed range of Figure 18 where it significantly underestimates the e-folding time; in the range of very low wind speeds, the

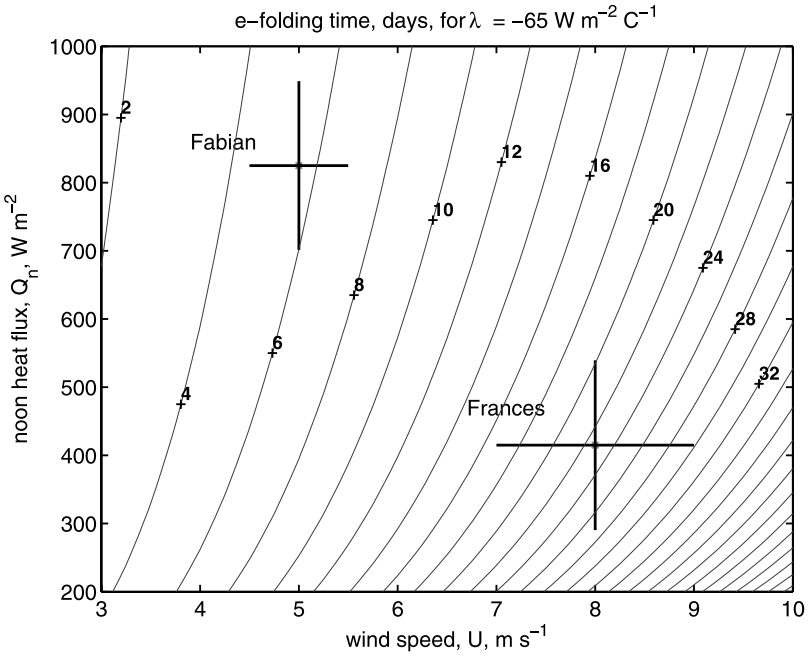


**Figure 18.** The solution equation (8) for e-folding time for a $\lambda$ appropriate to the late summer trade winds. Wind speed and wind stress of equation (8) are related by the neutral drag coefficient of *Fairall et al.* [2003]. The estimated wind speed and noon maximum heat flux for post-Fabian and post-Frances conditions are shown by the two sets of crossed error bars that represent the estimated uncertainty on wind speed and the noon heat flux (section 2.3).

scale analysis (8) predicts $\Gamma = 2$ days, where the numerical simulations indicate closer to 4 days. This low wind speed bias toward shorter $\Gamma$ stems from two simplifications of the scale analysis that act in the same sense: (1) the neglect of penetrating of solar insolation, which leads to excessive surface heating when the trapping depth is shallow, $D \leq 10$ m, and (2) neglect of the wind speed-dependence of $\lambda$, (3), which leads to a larger than simulated heat flux anomaly at low wind speeds. Both of these errors could be remedied in principle.

[48] There are no disposable constants in (8) which makes definite predictions or hindcasts of the e-folding time given two key pieces of data; the wind stress, which will be calculated from QuikSCAT estimates of wind speed noted already in section 2.3 and the *Fairall et al.* [2003] drag coefficient, and the noon maximum heat flux. The latter can be read from the numerical simulations (Figures 14 and 15, upper): $Q_n = 825 \pm 50$ W m$^{-2}$ and $415 \pm 130$ W m$^{-2}$ for Fabian and Frances, respectively. (Absent this kind of model data, one could estimate $Q_n$ as the noon maximum solar insolation less 100 W m$^{-2}$ to account for a nominal, posthurricane heatloss.) The uncertainties were estimated by propagating the uncertainty of cloud fraction through the insolation calculation (section 4.1) and are relevant when we compare the scale analysis to the observed e-folding times. The uncertainty on the estimated $Q_n$ is very large in the Frances case due to the large variation in cloud cover during the analysis period; the main source of uncertainty in evaluating (8) is nevertheless the wind speed as isolines of $\Gamma$ are quasi-vertical over most of Figure 18.

[49] Given the wind speed and heat flux estimates noted here and in section 2.3, the e-folding time computed from (8) is $\Gamma = 5.5 \pm 1$ days for the weather conditions post-Fabian and $\Gamma = 23 \pm 7$ days for weather conditions post-Frances (Figure 18). These are slightly less than the e-folding times found in the numerical simulations, $\Gamma = 7$ days for post-Fabian weather conditions and $\Gamma = 24$ days for post-Frances conditions of higher wind speed and greater cloud cover (section 4.1).

[50] The e-folding times computed from (8) are also within the (broad) range of e-folding times estimated from GOES and drifter SST observations of sections 3.2 and 3.3, $\Gamma = 5.5 \pm 1$ and $\Gamma = 20 \pm 10$, for Fabian and Frances, respectively (recall our reservations about the amplitude of warming in the Frances case, section 4.1, and which applies here as well). At the outset of this analysis we posed the question, why are the e-folding times markedly different between the Fabian and Frances cases?, and an interpretation of Figure 18 comes as close to an answer as we can offer. Most of the difference in the model-computed e-folding times can be attributed to the difference in wind speed (higher post-Frances). That is, even if the cloud cover and heat fluxes had been the same, the model-estimated e-folding times would still differ by a factor of about 3 due to the difference in wind speed (wind stress). This sensitive dependence upon wind speed follows directly from the wind stress dependence of the trapping depth, (5).

### 4.3. Connection With the Diurnal Cycle

[51] We noted in section 2.1 that the warming in a hurricane wake is modulated by the diurnal cycle of the upper ocean. The wake warming and diurnal cycle of SST are related in several respects but most directly insofar as both depend upon the amplitude of the diurnally varying

heat flux and the wind stress. In the PWP analysis, the amplitude of the diurnal cycle is estimated as [PWP, equation (17)]

$$T' = \frac{Q_n^{3/2}}{\tau} \frac{\left(\alpha g P_Q\right)^{1/2}}{\rho C_P^{3/2}}, \tag{9}$$

where all symbols are as defined in section 4.2 and having made the approximation $P_f = P_Q$ noted there as well. Thus the amplitude of the diurnal cycle depends upon $Q_n$ and $\tau$, but not separately upon the slowly varying heat flux anomaly $\delta Q$ in the way that $\Gamma$ does. That aside, larger $T'$ would generally be expected to go along with smaller $\Gamma$, which is what we found comparing the Fabian and Frances cases and within the extensive Frances drifter data set (Figure 12).

[52] We can attempt to use the observed amplitude of the diurnal cycle as a proxy for, e.g., the wind stress, $\tau$. Solving (9) for $\tau$, and then substituting into (8) gives a very simple result,

$$\Gamma = \frac{Q_n}{\lambda T'} P_Q. \tag{10}$$

if the diurnal cycle amplitude $T'$ can be presumed known. Substitution of the ensemble-averaged value of $T'$ (sections 2.1 and 3.2) into (10) along with the $Q_n$ noted above, we calculate that $\Gamma \approx 5$ days in the Fabian case and somewhat longer, 10 days in the Frances case. The former estimate of $\Gamma$ is quite good and seems to indicate consistency between the scaling analysis used here and the observed wake warming and diurnal warming. The latter estimate of $\Gamma$ is too small, as if the ensemble-average $T'$ was too large. We suspect that the discrepancy may follow in part from the large standard deviation of $T'$ (comparable to the mean) which in turn followed from the large day-to-day variation of especially the cloud cover (Figure 6); from (9), a day-to-day varying $Q_n$ will produce a larger average $T'$ than would the average $Q_n$. Thus the analysis that leads to (8) and (10) has taken account of a first order property of the surface heat flux, that it varies diurnally, but has taken no account of the day-to-day variation of $\tau$ or of $Q_n$.

## 5. Summary and Remarks

### 5.1. Main Results

[53] There are four main results or conclusions from this study. The first is the more or less direct observation that SST in the cool wake of a moving hurricane will warm toward prehurricane (or equilibrium) SST on a timescale of about 5 to 20 days (e-folding time of the cool anomaly). From our experience analyzing a number of other western North Atlantic hurricanes from the 2003 and 2004 seasons, we find that the shorter timescale is the more common. However, we have also seen an example from early fall 2004 (Hurricane Jeanne, 2004; see the auxiliary material) in which a cool wake persisted with little change for several weeks until it was finally engulfed by the cooling phase of the seasonal cycle. Thus, the warming of SST in the cool wake of a hurricane can be and often is fairly rapid; it is most certainly variable from case-to-case.

[54] The second result is that this wake warming process is mainly a local phenomenon that is driven by air-sea fluxes (“local” meaning depth and time dependent). The evidence leading to this conclusion is that (1) the cool wakes faded away while remaining almost in place. (2) The areal integral of the cool anomaly clearly decreased. (3) The rate of warming was positively correlated with the amplitude of the cooling, i.e., the central and coolest part of a wake warmed the fastest, in an absolute sense. (4) The warming was most rapid during periods of clear skies and light winds, the same conditions that lead to a large amplitude diurnal cycle of SST.

[55] We have inferred that the air sea heat flux that causes the warming can be estimated from the change in the heat flux loss terms associated with the anomaly of SST (section 4.2.1). For nominal trade wind conditions, this implies an anomalous heat flux of about $-65$ W m$^{-2}$ per °C of the SST anomaly. For a typical cool wake, $\delta T = -2$°C SST, this gives a (positive) heat flux of only about 130 W m$^{-2}$, which nevertheless appears to be sufficient to warm the sea surface at an appreciable rate. If indeed the observed SST warming is due to this modest heat flux, then the heat flux must be absorbed within a rather thin, O(10 m), surface layer. What sets this thickness scale?

[56] The third result is the model-derived inference that the thickness of the warm layer is proportional to the trapping depth of the diurnal warm layer. Under fair, trade wind weather conditions, this can indeed be rather thin, O(10 m), but dependent upon the noon maximum heat flux and the wind stress magnitude (section 4.2.2). Thus, in the days or weeks after a hurricane passage, the out of balance surface heat flux is absorbed and stored within an ocean surface layer whose thickness is set by the largest value of the warming (stabilizing) heat flux associated with the diurnal cycle.

[57] From these first three results it is only a short step to the fourth result, a simple, closed solution (essentially a scale analysis) for e-folding time, $\Gamma \propto \tau/\lambda\sqrt{Q_n}$. This modeled e-folding time shows explicit dependence upon both the slowly varying heat flux associated with the SST anomaly, $\lambda$, and the variance of the heat flux, represented by the noon maximum, $Q_n$. This solution gives more or less reasonable results in the two cases considered and suggests that the much longer e-folding time found in the Frances case was due mainly to the somewhat higher wind speed in that case.

### 5.2. Cautionary Remarks

[58] It goes almost without saying that the present, two cases of wake warming (with incomplete atmospheric data) do not constitute a convincing test of (8), which we view as a hypothesis, and not a proven result. A rigorous test of (8) would require hourly atmospheric measurements of air temperatures and radiative fluxes and in situ ocean data sufficient to define the temperature profile over roughly the upper 40 m with depth roughly resolution of several meters. The most important and readily falisifiable prediction of the modeling results shown here is that a rapidly warming SST (as in the Fabian case) will be representative of a thin, O(10 m), ocean surface layer.

[59] But whether (8) proves to be mostly right or not, we know for sure that it is not general; there is a sense in which

it is both incomplete and fragile. It is incomplete because the heat flux anomaly was computed on the assumption that the variable air-sea temperature difference was due to the cool anomaly of SST alone, i.e., that air temperatures remained constant. But suppose that air temperature declined significantly after the passage of a hurricane; the net heat loss would then be significantly underestimated by our heat flux anomaly (3) and there might be no wake warming at all despite significant solar insolation and fair winds. The signature of this would be a slow cooling of the far field (outlying) SST, as seems to occur in the late-season Hurricane Jeanne (2004) case noted above. In principle, the possibility of a changing air temperature could be incorporated into (3) and (8), but if sufficient detail of the surface atmosphere is known, then a numerical upper ocean model would be a more appropriate tool. Our result (8) is fragile because it applies only in the idealized condition of fair, homogeneous trade wind weather. Fair weather often does follow a hurricane, but during the active 2003 and 2004 North Atlantic hurricane seasons, the frequent occurrence of hurricanes limited the duration to no more than a week or two. Thus (8) appears to give a reasonably good account of the warming rate for about 5 days post-Fabian or up until the onset of higher winds associated with Hurricane Isabel. Beyond that time our analysis is not so much wrong (though it clearly is) as it is inapplicable.

### 5.3. Closing Remarks

#### 5.3.1. Heating and Cooling

[60] This analysis serves to highlight several of the qualitative physical differences in the upper ocean's response to heating versus cooling and wind mixing. Perhaps the most important, generalizable result of this analysis is that under sustained heating conditions, the variance of the heat flux, together with the wind stress, is likely to determine the thickness of the ocean surface layer that absorbs a warming heat flux. This has some significance for modeling of SST on climate or long timescales; surface fluxes that are averaged over a day or more will not be equivalent physically to the corresponding instantaneous (or hourly, say) heat flux, when the heat flux includes large amplitude diurnal variation of the solar insolation. To say it a little differently, we are dubious that a consistent model of the hurricane wake warming process can be constructed on the basis of the daily (or longer) averaged surface heat flux alone, while ignoring the diurnal variation of solar insolation. Under conditions of sustained cooling this is not expected to be true.

[61] In the strong heating conditions of a hurricane wake, the warming rate appears to be determined by surface fluxes of heat (buoyancy) and the wind stress alone; the initial subsurface stratification is not important, in part because density is homogenized to depths of O(50 m) or more by the hurricane winds. The effect of strong surface heating combined with the dependence of the net heat flux upon SST is then to and produce a horizontally homogeneous SST field [*Katsaros and Soloviev*, 2004]. However under conditions of cooling and wind-mixing, just the opposite will hold; vertical mixing will uncover existing subsurface, horizontal variation of stratification, as in the drifter-observed SST response to the higher winds associated with Hurricane Isabel (2003) (Figure 4). The SST response to cooling and wind-mixing thus depends upon the surface fluxes and the initial stratification. For that reason, our result (8) would not be appropriate for predicting the evolution of a warm SST anomaly, even if the anomalous heat flux followed (3), since it takes no account of the initial thickness of an SST anomaly.

#### 5.3.2. Local and Nonlocal

[62] While the evidence developed here suggests that the dominant process of SST warming in a hurricane cool wake is a local, surface flux-driven process, it is very unlikely that this is the sole process that modifies a hurricane wake, even at the sea surface. We suspect that the local dynamics described here may not be relevant at all for depths greater than about 25 m. From the displacement of surface drifters it is apparent that the prehurricane, ocean mesoscale will stir a hurricane cool wake and deform the wake significantly on timescales of a week or more. There may also occur a wide range of air-sea interaction processes that owe their existence to the horizontal variation of density and current imposed by the hurricane and so are essentially nonlocal.

##### 5.3.2.1. Baroclinic Instability

[63] The cool wake has a subsurface signature extending to roughly 100 m and that represents a significant reservoir of available potential energy. The wake is very likely to be unstable to small horizontal-scale, surface trapped, baroclinic instability [*Boccaletti et al.*, 2007]. Growing instabilities will act to disperse the wake on a timescale of several weeks (B. Fox-Kemper and R. Ferrari personal communication, 2007) and induce SST variability on a spatial scale of several to 10 km. One effect of the wake dispersal is to restratify the vertically homogeneous mixed layer.

##### 5.3.2.2. Planetary Boundary Layer

[64] The horizontal variation of SST across a hurricane wake must cause a significant horizontal variation in the stability of the planetary boundary layer associated with the air-sea temperature difference, and so cause horizontal variations in the wind stress resulting from a given (and presumably unaffected) geostrophic wind. *Lin et al.* [2003a] indicate wind speed variation of about 1 m $s^{-1}$ per degree C. In this study we have taken the wind from satellite observations and moreover, spatially averaged observations. This may tend to overestimate the wind stress on the coldest and most stable (atmospheric surface layer) part of the wake, and thereby lead to an overestimate of the e-folding time.

##### 5.3.2.3. Nonlocal Ekman Layer Dynamics

[65] The Ekman layer transport within a horizontally varying surface layer is likely to induce vertical mixing in regions where the surface wind-driven flow has a component along the SST gradient, and, like the baroclinic instability noted above, may act to restratify the mixed layer in regions where the opposite sign of advection obtains [*Thomas and Lee*, 2005]. A hurricane's cool wake appears to be a natural laboratory for these and other nonlocal processes of upper ocean dynamics and air-sea interaction.

[66] **Acknowledgments.** JFP, JM, and PPN all thank the U. S. Office of Naval Research for generous support during the time of this analysis. The success of the CBLAST field programs was made possible by the skilled assistance of the U. S. Air Force Reserve 53rd Weather Reconnaissance Squadron and our CBLAST colleagues, especially Peter Black, Shuyi Chen, and Eric D'Asaro. Many of the drifters used in the Frances study

were deployed as part of an operational hurricane forecasting program sponsored by the U. S. Naval Oceanographic Office. Our thanks also to Roger Goldsmith of WHOI for help with graphics, to Mike Caruso of WHOI for advice regarding satellite data, and to NASA/JPL for the excellent POET data server. Tom Farrar of WHOI is thanked for his insightful suggestions on a draft manuscript.

## References

Black, P. G., E. A. D'Asaro, W. M. Drennan, J. R. French, P. P. Niiler, T. B. Sanford, E. J. Terrill, E. J. Walsh, and J. A. Zhang (2007), Air-sea exchange in hurricanes: Observations from the Coupled Boundary Layer Air-Sea Transfer experiment, *Bull. Am. Meteorol. Soc.*, *88*, 357–374.

Boccaletti, G., R. Ferrari, and B. Fox-Kemper (2007), Mixed layer instabilities and restratification, *J. Phys. Oceanogr.*, *37*, 228–2250, doi:10.1175/JPO3101.1.

Bunker, A. F. (1976), Computations of surface energy flux and annual air-sea interaction cycles of the North Atlantic ocean, *Mon. Weather Rev.*, *104*(9), 1122–1140.

Cornillon, P. L., R. S. Stramma, and J. F. Price (1987), Satellite measurements of sea surface cooling during Hurricane Gloria, *Nature*, *328*, 373–375.

D'Asaro, E., T. B. Sanford, P. P. Niiler, and E. J. Terrill (2007), Cold wake of Hurricane Frances, *Geophys. Res. Lett.*, *34*, L15609, doi:10.1029/2007GL030160.

Emanuel, K. A., C. DesAutels, C. Holloway, and R. Korty (2004), Environmental controls on tropical cyclone intensity, *J. Atmos. Sci.*, *61*, 843–858.

Fairall, C. W., E. F. Bradley, J. E. Hare, A. A. Grachev, and J. B. Edson (2003), Bulk parameterization of air-sea fluxes: Updates and verification of the COARE algorithm, *J. Clim.*, *16*, 571–591.

Gentemann, C. L., C. J. Donlon, A. Stuart-Menteth, and F. J. Wentz (2003), Diurnal signals in satellite sea surface temperature measurements, *Geophys. Res. Lett.*, *30*(3), 1140, doi:10.1029/2002GL016291.

Katsaros, K. B., and A. V. Soloviev (2004), Vanishing horizontal sea surface temperature gradients at low wind speeds, *Boundary Layer Meteorol.*, *112*, 381–396.

Lin, I., W. T. Liu, C. Wu, J. C. H. Chiang, and C. Sui (2003a), Satellite observations of modulation of surface winds by typhoon-induced upper ocean cooling, *Geophys. Res. Lett.*, *30*(3), 1131, doi:10.1029/2002GL015674.

Lin, I., W. T. Liu, C. Wu, G. T. F. Wong, C. Hu, Z. Chen, W. Liang, Y. Yang, and K. Lee (2003b), New evidence for enhanced ocean primary production triggered by tropical cyclone, *Geophys. Res. Lett.*, *30*(13), 1718, doi:10.1029/2003GL017141.

Lin, I. I., C. C. Wu, K. A. Emanuel, I. H. Lee, C. R. Wu, and I. F. Pun (2005), The interaction of Supertyphoon Maemi (2003) with a warm ocean eddy, *Mon. Weather Rev.*, *113*, 2635–2649.

Nelson, N. B. (1998), Spatial and temporal extent of sea surface temperature modifications by hurricanes in the Sargasso Sea during the 1995 season, *Mon. Weather Rev.*, *126*, 1364–1368.

Price, J. F. (1981), Upper ocean response to a hurricane, *J. Phys. Oceanogr.*, *11*(2), 153–175.

Price, J. F., R. A. Weller, and R. Pinkel (1986), Diurnal cycling: Observations and models of the upper ocean response to diurnal heating, cooling and wind-mixing, *J. Geophys. Res.*, *91*, 8411–8427.

Sanford, T. B., J. F. Price, J. B. Girton, and D. C. Webb (2007), Highly resolved ocean response to a hurricane, *Geophys. Res. Lett.*, *34*, L13604, doi:10.1029/2007GL029679.

Sriver, R. L., and M. Huber (2007), Observational evidence for an ocean heat pump induced by tropical cyclones, *Nature*, *447*, 577–580.

Stramma, R. S., P. Cornillon, and J. F. Price (1986), Satellite observation of sea surface cooling by hurricanes, *J. Geophys. Res.*, *91*, 5031–5035.

Thomas, L., and C. M. Lee (2005), Intensification of ocean fronts by downfront winds, *J. Phys. Oceanogr.*, *35*, 1086–1093.

Wentz, F. J., C. Gentemann, D. Smith, and D. Chelton (2000), Satellite measurements of sea surface temperature through clouds, *Science*, *228*, 847–850.

J. Morzel, CoRA Division, NorthWest Research Associates, 3380 Mitchell Lane, Boulder, CO 80301, USA.

P. P. Niiler, Scripps Institution of Oceanography, University of California, San Diego, 9500 Gilman Drive, La Jolla, CA 92093, USA.

J. F. Price, Physical Oceanography Department, Woods Hole Oceanographic Institution, Woods Hole, MA 02543, USA. (jprice@whoi.edu)